Available online at www.sciencedirect.com

jmr&t Journal of Materials Research and Technology

journal homepage: www.elsevier.com/locate/jmrt

Original Article

The development of miniature tensile specimens with non-standard aspect and slimness ratios for rapid alloy prototyping processes

Lintao Zhang *, *Will Harrison*, *Mazher A. Yar*, *Stephen G.R. Brown*, *Nicholas P. Lavery*

Future Manufacturing Research Institute, College of Engineering, Swansea University, Bay Campus, Fabian Way, Swansea, SA1 8EN, UK

ARTICLE INFO

Article history:
Received 13 June 2021
Accepted 6 September 2021
Available online 11 September 2021

Keywords:
Miniaturized mechanical test
Miniaturized tensile test (MTT)
Miniaturized tensile specimen (MTS)
Specimen size effects
Slimness ratio

ABSTRACT

This work aims to evaluate the use of miniaturized tensile specimen (MTS) to characterise the mechanical properties of alloys developed through rapid alloy prototyping (RAP), where high throughput tests are required on relatively small amounts of material. Tensile tests were conducted at a variety of strain rates and with increasingly smaller specimen sizes, ranging from larger specimens conforming to ASTM/ISO standards, down to small non-standard specimens. The gauge lengths of the specimens ranged from 50 to 80 mm for the standard specimens down to 5–10 mm for the non-standard specimens. To generalize the non-standard MTS designs, three alloys, DP800, DP600 and 316L stainless steel, were adopted. The results obtained from non-standard designs were compared with those from standard designs. The results show that non-standard designs can give repeatable results for yield strength (YS), ultimate tensile strength (UTS) and uniform elongation (e_U). The maximum result differences of YS, UTS and e_U are 7.37%, 7.71% and 11.9%, respectively, for DP alloys comparing standard and non-standard dimensions. These values are 13.56%, 14.03% and 19.5%, respectively 316L steel. The total elongation (e_f) increases as the specimen dimension decreases. The geometrically dependent constants (n) are 0.2, 0.31 and 0.11 for DP800, DP600 and 316L, respectively. However, the Young's modulus is hard to determine precisely from the miniaturized designs. The conclusion from this work is that miniaturized tensile testing can be used with confidence as a high throughput means of predicting standard mechanical properties across a range of steels.

1. Introduction

Tensile testing is a mechanical test used to determine the uniaxial mechanical properties of materials under loading with different strain rates. The results obtained from tensile tests can provide basic material properties such as yield strength (YS), ultimate tensile strength (UTS) and elongation information. The first concept of the tensile test was developed by Petrus van Musschenbroek using his 'lever testing

* Corresponding author.
E-mail address: L.Zhang@Swansea.ac.uk (L. Zhang).
https://doi.org/10.1016/j.jmrt.2021.09.029

machine' [1]. Tensile test set-ups comprise a tensile loading machine, extensometers (either clip-on mechanical extensometers or non-contact systems such as video extensometers) and tensile test specimens.

A tensile test specimen usually has a 'dog-bone' shape and one of the first standards for tensile testing of metallic materials, BS18, was published by the British Engineering Standard Association in 1904 [2]. In recent years, there is a trend to miniaturize tensile specimen dimensions often referred to as Miniaturized Tensile Test (MTT) technology. There are several possible motivations: Insufficient material for standard samples (e.g., nanomaterials), testing of small amounts of in-service material (e.g., power generation equipment), new alloy development processes (e.g., rapid alloy prototyping).

The quantity of material required from a Rapid Alloy Prototyping process ranges through milligrams, grams, kilograms to tonnes, depending on the development stage of the alloy, with more material needed at the later industrial trials which might result in new alloys every few years. The transition from laboratory to industrial RAP routes is dictated by the material properties needed at any given stage. For strip steels [3,4], particularly when tensile strength increases are targeted, traditionally the smallest laboratory scale will require kilograms for compositional accuracy in cast ingots and sufficient material for hot and cold rolling mills. Even at this scale RAP has given alloy development a six fold increase in speed [4]. Recently, big efforts are being made to further increase RAP speed by reducing the material down to 20–140 g cast per composition [5], with a target of 100 compositions being made and tested per week. Central to achieving this goal is a ten times reduction of the tensile test specimen, allowing for more tests to be done quicker, but with well-known scaling factors to accurately predict the tensile properties of standard specimens.

The usual strategy to design miniaturized tensile specimen (MTS) is either to scale down the dimensions from the existing standard dimensions or make further modifications after scaling [6]. As the specimen size decreases, the 'size effect can occur. If the differences between results for MTS and standard specimens are in an acceptable range, e.g., −15%–15% then this indicates that the results obtained from MTS are a good estimate of the mechanical properties. However, with further decreases in specimen thickness, down to perhaps 6 to 10 times the average grain size, then the tensile test results of MTS no longer reflect bulk material properties [6]. Interestingly, in another study using 316L stainless steel [7] it is suggested that yield strength can be measured by MTS if the ratio of specimen thickness to the grain size is 3 or higher. However, for UTS measurement this ratio value should ideally be greater than 7. Zhu et al. studied these specimen thickness to average grain size ratios in the range of 2.7–13.7 under different strain rates for pure titanium foil [8]. The results indicated that the flow stress decreased as the ratio was decreased, and this is independent of the strain rate.

The Aspect Ratio, *AR* (the specimen thickness to width ratio, although some researchers define AR as the ratio of width to thickness) has also been considered [9]. *AR* is important for this study since specimen thickness is fixed by the manufacturing process and cannot be adjusted. Increasing *AR* values can result in the reduction of necking angle. The necking angle variation was further explained by Mikkelsen through numerical simulation [10,11]. Similar results were obtained in the work of Kohno et al. [12]. The total elongation increases with increasing *AR* values. The reason for this is due to the differences in the necking behaviour [10].

The slimness ratio (ratio of gauge length to square root of cross-section area) for standard bars is 5.65 according to the ISO 6892−1:2016 standard [8]. This value can also vary from 4 to 11.3 [13] and possible constant values 4 or 5 for the standard tensile bar [14,15]. All these values are suggested by the different standards, some are less strict ASTM in the US with 4, and others are stricter such as the German DIN standard requiring a slimness ratio above 11. The greatest effect of the *AR* is on the elongation to failure [6], but the Bertella-Oliver formula in Eq. (1) can be used to convert between standards with relative confidence. Kashaev et al. developed an MTS method ($AR = 0.25$) and conducted tensile tests for Inconel 625, 718 and Ti–6Al–4V alloys [16]. The results indicated that this ratio could give consistent results with acceptable differences between MTS and standard specimens. Zhao et al. designed an MTS with a larger gripping tab, having a gauge length 1 mm and *AR* values varying from 0.125 to 0.5 [11]. The design was used to study the size effect on ultra-fine-grained Cu. It showed that the shorter and thicker specimens tended to give higher elongations. Another MTS was designed by Dzugan et al. with an *AR* value of 0.33 which was used to test DC01 steel [17]. Yang et al. designed an MTS with an *AR* value of 0.4 to measure the material properties of a CrMoV steel weldment [18]. Apart from dog-bone shapes, some other shapes were also developed, for example, bow-tie shapes [19] and dumb-bell shapes [20]. The results indicated that only a 5% deviation in results was found when compared to the standard specimen.

The authors were unable to find any standardization of mini tensile specimen design or testing standards, other than cases using proportional sizing of standard specimen geometries. To help ensure that MTT results can represent bulk material properties there are several general guidelines. The ratio of MTS thickness to average grain size should larger than 6 (but may vary with material). The *AR* value of the MTS should be greater than 0.2 and the slimness ratio should be around 5.65 (ISO 6892−1:2016. However, these guidelines lead to several questions:

1. Before using MTT to characterize novel alloys generated using rapid alloy prototyping (RAP), the validity of the method applied to existing grades must be determined [5]. What level of dimension of MTS should be?
2. Will the proposed non-standard MTS work for different alloys?
3. Will the MTS test results still represent the bulk material properties if the slimness ratio is reduced, even beyond the current standard suggested range?
4. When using new MTS designs, how does the test strain rate affect the MTT results?

Tackling these open questions is the main task of the current research.

2. Materials and methods

2.1. Alloys selected and miniaturized tensile specimen designs

Three alloys were selected: DP800, DP600 and 316L stainless steel, respectively. The chemical compositions of the selected alloys are summarized in Table 1.

The reason for this selection is that DP600 and DP800 are grades of current interest [5] and 316L was added to provide a wider range of tensile properties, 316L exhibits a higher rate of work hardening and higher ductility. DP600 and DP800 are rolled steel products but for contrast the 316L samples were additively manufactured (via Laser Powder Bed Fusion or LPBF) as the interest in this work is the dimensional scaling effects of specimen sizes for different alloys and processes. Figure 1 shows the specimen dimensions selected in the current research.

Among these dimensions, A80, A50 and ASTM25 are standard dimensions used as benchmarks. Two non-standard MTS designs were also proposed, called Mini1 and Mini2, respectively. According to the basic strategies of designing MTS, the parallel section length (L_c) of Mini1 was scaled down, by a ratio of 2, from the ASTM subsize standard. Mini2 is a further scaled down version of Mini1. Compared to the SS-series [21] (generated in Japan in 1980–1990s and gripped with pins), these two non-standard MTS have similar parallel length values (Mini1 to SS2 and Mini2 to SS3), however they have different parallel width and thickness values. For both Mini1 and Mini2, the tab sections were enlarged to ensure a firm grip during testing. This is different to the pin-gripped designs in the SS-series. The detailed dimensions of different designs are summarized in Table 2.

Compared with the general guidelines for designing MTS (mentioned in Sec.1), the ratio of specimen thickness to the average grain size of the selected alloys is in the order of hundreds [22]. For Mini2, the *AR* values range from 0.6 to 0.8, larger than the critical *AR* value of 0.2 [9, 12]. The slimness ratios of Mini2 range from 2.8 to 3.23. These values are smaller than 5.65 (ISO 6892–1:2016) and 3.2 to 14.1 (ASTM E8M–16 standard). To determine the isotropic features of the alloys, longitudinal (L-Bar, 0°) and transverse (T-Bar, 90°) bars were manufactured for DP800 and DP600 representing specimens where the angles, between the rolling and pulling directions, are 0° and 90°, respectively.

The electric discharge machining (EDM) method was used to cut DP alloy specimens. The Laser Powder Bed Fusion systems (Renishaw AM400) AM method was used to additively manufacture 316L stainless steel tensile specimens. The mechanical properties of 316L manufactured using this method have been well characterized [23,24]. These samples were made in the vertical orientation (normal orientation to the powder bed) with a laser power of 195 W, a point distance of 60 μm, an exposure time of 80 μm and a hatch spacing of 110 μm. A meander hatch pattern was used with 67° between layers and the specimens were tested without heat treatment.

2.2. Experiment facilities

The same uniaxial tensile machine Tinius-Olsen H25KS was used to conduct the experiments for all specimen sizes. The machine has a 25 kN force capacity with an accuracy of ±0.5% of applied load from 2 to 100% of the load cell capacity and ±1% down to 1% of the load cell capacity. For specimens with gauge lengths below 20 mm it becomes increasingly difficult to use the traditional clip-on extensometers. In the current research, a video extensometer (XSight 9MPX) was adopted to capture the strain for all sizes of tensile specimens. To ensure accurate specimen dimensions and exclude the influence of any surface scratches, edge tears or residual stress distortions arising from machining, the specimens were first examined using a Shadowgraph machine before tensile testing. Mitutoyo SJ-210 surface roughness tester was used to evaluate the surface roughness of the tensile specimen. The arithmetic mean deviation of the profile (R_a), the root-mean-square deviation of the profile (R_q) and the ten-point height of irregularities (R_z) were measured and summarized in Table 3.

The DP800 and DP600 tensile specimen were manufactured through EMD method, which is a high precision (the maximum roughness of 1 μm), gentle cutting process (introduces little work hardening into the specimen, compared to computer numerical control machining or lathing) which results in smooth edges, from the rolled sheet steels. Therefore, the low values of roughness are expected and no further finishing was required. Another reason for not applying any additional finishing to the specimens is that the industrial tensile tests are carried out on the large A80 specimen with the strip steel in the same condition. The additively made (3D printed) 316L bars for the current work, were rougher than the rolled steel, as would be expected, with R_a in the region of 4–5 μm. In the authors' experience of tensile testing of AM alloys, particularly of ductile alloys such as 316L the effect of surface roughness is relatively minor compared to fatigue testing [24].

Initially, a fixed pulling velocity of 1 mm/min was adopted to for all specimens. The correspondent strain rates, normalized by L_0, for each size specimen are 2.1 $\times 10^{-4}$ s^{-1}, 3.3 $\times 10^{-4}$ s^{-1}, 6.7 $\times$ 10^{-4} s^{-1}, 1.7 $\times$ 10^{-3} s^{-1} and 3.3 $\times$ 10^{-3} s^{-1} for specimen dimensions A80, A50, ASTM25, Mini1 and Mini2, respectively. Before conducting the experiments, for all specimens, the test piece widths (b_0) and thicknesses (a_0) were determined as the average of 3–5 measurements along each sample.

Table 1 – Chemical compositions for DP800, DP600 and 316L stainless steel (% weight).

	C	Si	Mn	P	S	Ni	Cu	Cr
DP800	0.136	0.249	1.77	0.011	0.0027	0.018	0.024	0.558
DP600	0.098	0.244	1.705	0.015	0.004	0.023	0.018	0.548
316L	0.03	1.0	2.0	0.04	0.03	10.0–14.0	–	16.0–18.0

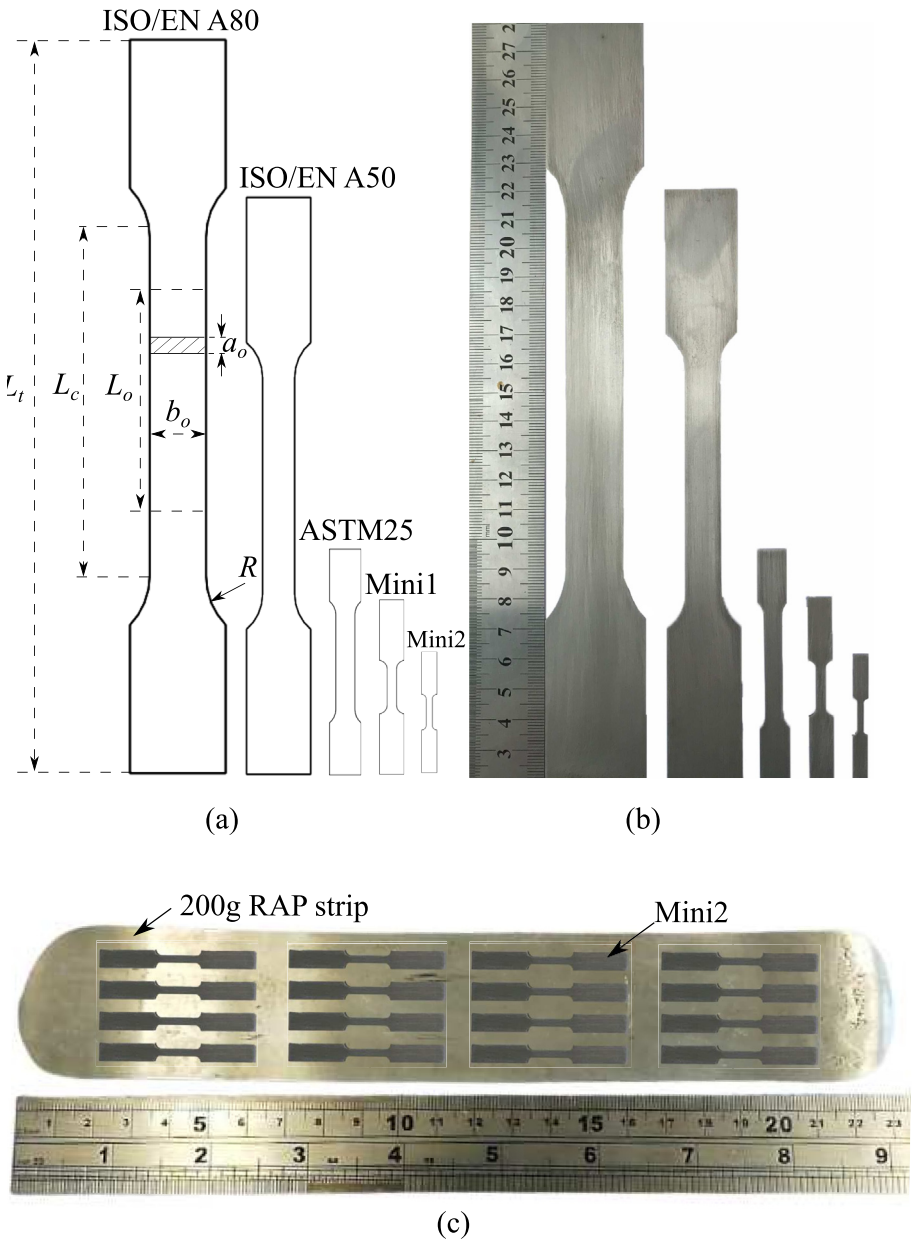

Fig. 1 – CAD drawings (a) and photos (b) of different tensile test specimens. L_t, L_c, L_o, b_0, R and a_0 denote the total length, the parallel section length, the gauge length, the original width, the shoulder radius and the original thickness of the test piece, respectively. Mini1 and Mini2 are designed non-standard tensile specimens. (c) Planning of Mini2 specimen on the 200g RAP strip.

3. Results and discussion

3.1. *Repeatability of miniaturized tensile specimens testing results*

Figure 2 shows the engineering stress–strain curves for DP800, DP600 and 316L alloys for Mini1 (*Top*) and Mini2 (*Bottom*) for L-bar (Longitudinal) and T-bar (Transverse) specimens.

The different family of curves show that the results, obtained from the non-standard Mini1 and Mini2 design, for each of the materials tested are in the target ranges. DP800 and DP600 have the highest strength of the order of 800 and 600 MPa, respectively. The increase in DP800 strength, compared to DP600, is because of the increased proportion of martensite/bainite compared to ferrite [25]. For 316L steel, the highest strength is around 450 MPa and the value is a bit lower than the expected value 500 MPa. This is may due to the

Table 2 – Tested tensile bar dimensions. L_t, L_c, L_o, b_0, R and a_0 denote the total length of test piece, parallel length, gauge length, original width of the parallel length of a flat test piece, the shoulder radius and the thickness of the bar, respectively. Slimness ratio and aspect ratio are defined as $\frac{L_o}{\sqrt{a_0 \cdot b_0}}$ and $\frac{a_0}{b_0}$. No. denotes the number of the tests for each dimension and material (for DP800 and DP600, the value is the total number of L-bar and T-bar).

		L_t (mm)	L_c (mm)	L_o (mm)	b_0 (mm)	R (–)	L_o/L_c (–)	L_o/b_0 (–)	$(L_c\text{-}2b_0)/L_0$ (–)	a_0 (mm)	Slimness ratio (–)	AR (–)	No. (–)
A80	DP800	260	120	80	20	25	0.67	4	1	1.2	16.33	0.06	2
	DP600									1.6	14.14	0.08	2
	316L									1.3	15.69	0.07	3
A50	DP800	200	75	50	12.5	15	0.67	4	1	1.2	12.91	0.10	6
	DP600									1.6	11.18	0.14	6
	316L									1.3	12.4	0.10	3
ASTM25	DP800	76	32	25	6	6	0.78	4.17	0.8	1.2	9.32	0.20	6
	DP600									1.6	8.07	0.27	6
	316L									1.3	8.95	0.22	3
Mini1	DP800	60	12.5	10	3	3	0.8	3.33	0.65	1.2	5.27	0.4	8
	DP600									1.6	4.56	0.53	6
	316L									1.3	5.06	0.43	6
Mini2	DP800	41	9	5	2	1.5	0.56	2.5	1	1.2	3.23	0.6	17
	DP600									1.6	2.80	0.8	6
	316L									1.3	3.10	0.65	4

manufacturing method of the 316L steel MTS: the additive manufacture method may cause some internal defect, e.g. porosity, and therefore affect the test result [24]. It can also be seen that the total elongation values (e_f) for the AM-manufactured 316L steel shows relatively more scatter across the samples, this is discussed later. Some variation in total elongation is observed but this is common due to the nature of post-necking behaviour.

The results also indicate that the MTS designs, Mini1 and Mini2, can provide repeatable tensile results. These consistent tensile test outputs can be used to compared with benchmark values (results obtained from the standard specimens) to evaluate the effectiveness of Mini1 and Mini2.

Table 3 – A summary of R_a, R_q and R_z values for DP800, DP600 and 316L tensile specimen, respectively. RD TD and PD stand for rolling, transversal and pulling directions, respectively.

			Test 1	Test 2	Test 3
DP800	RD	R_a (μm)	0.690	0.727	0.730
		R_q (μm)	0.838	0.870	0.892
		R_z (μm)	3.723	4.170	3.907
	TD	R_a (μm)	0.681	0.692	0.707
		R_q (μm)	0.835	0.840	0.854
		R_z (μm)	3.553	3.721	4.097
DP600	RD	R_a (μm)	0.740	0.620	0.744
		R_q (μm)	0.898	0.773	0.894
		R_z (μm)	3.726	3.624	4.189
	TD	R_a (μm)	0.639	0.789	0.744
		R_q (μm)	0.798	0.967	0.928
		R_z (μm)	3.938	4.627	4.412
316L	PD	R_a (μm)	5.307	4.862	5.907
		R_q (μm)	6.663	5.875	7.037
		R_z (μm)	29.490	25.471	27.352
	TD	R_a (μm)	5.097	4.449	4.886
		R_q (μm)	6.224	5.733	6.005
		R_z (μm)	24.727	25.407	25.000

3.2. *Strain rate effect*

To evaluate the effect of strain rate within the practical test range a second series of tests were performed. Different displacement rates were used for Mini1 and Mini2 specimens. Figure 3 shows the influence of the strain rate on the values of YS, UTS, e_U, e_f and fracture time (t_f), respectively.

For both the Mini1 and Mini2 tests the results indicate that the YS and UTS values tend to increase with increasing strain rate. However, these differences are less than 5% in the current strain rate range. This trend has also been reported for aluminium alloys and low carbon steels at room temperature [26]. Furthermore, DP780 and DP600 present similar trend in the work of Cavusoglu et al. [27] in the strain rate range from 1 $\times 10^{-3}$ to 6 $\times 10^{-2}$. However, it is noticeable that the fracture time (t_f) increases significantly as the strain rate is decreased. For a RAP process a fixed pulling velocity of 1 mm/min is advantageous because it allows many tests to be scheduled and carried out rapidly.

3.3. *Young's modulus comparison*

Figure 4 shows the calculated Young's Modulus (YM) for DP800, DP600 and 316L from the tensile tests undertaken in accordance with the ASTM-E8 standard [15], using both the standard and non-standard specimen geometries, but complying to all other aspects of the standard, such as test speed and extensometer classes.

The ASTM-E8 standard aims to ensure accurate and repeatable determination of tensile properties, not elasticity moduli, and requires a full displacement through to specimen failure. The large A80 sample geometry gives values of the Young's modulus which fall within the range of expected values 180–225 GPa [28], but the non-standard MTS give much lower values and higher variance than those from the standard specimens. The 3D printed 316L specimens which should have a Young's modulus of 200 GPa, gives significantly lower

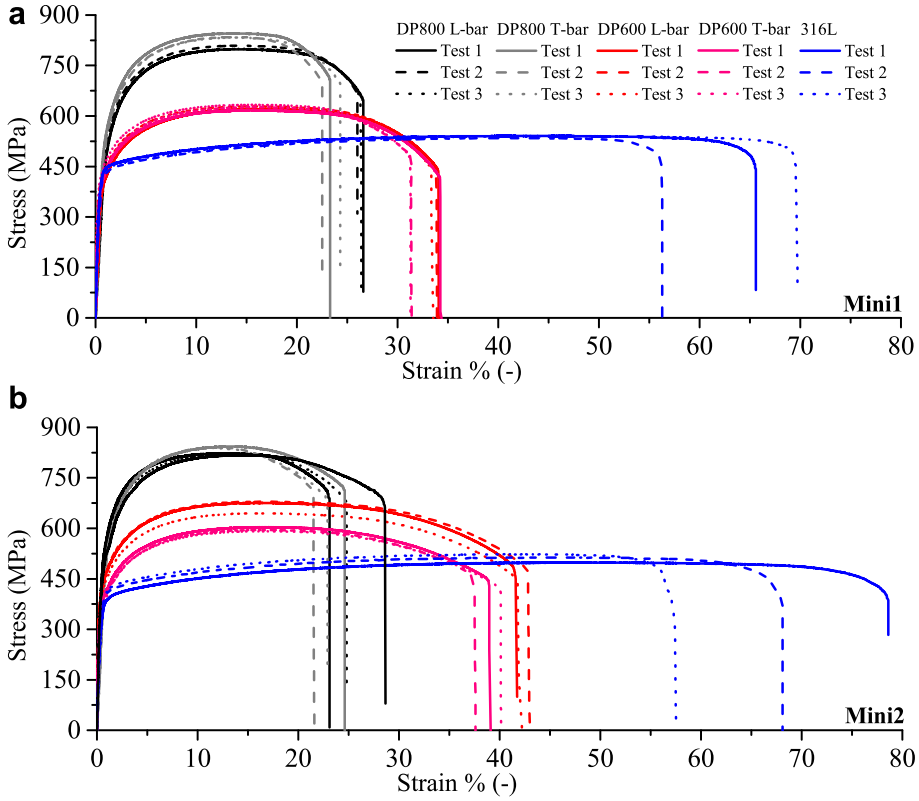

Fig. 2 – Stress–strain curves of selected alloys for Mini1 (*Top*) and Mini2 (*Bottom*). L-bar and T-bar denote the angle, between the rolling and the pulling directions, are 0° and 90°, respectively. The non-standard Mini1 and Mini2 designs can provide relative consistent results for the selected alloys.

values even for the large A80 specimen, but with similar variances across the different specimen geometries. The lower modulus of the vertically printed specimens is thought to be due to a combination of variable porosity in the build direction and residual stress, as the parts were neither stress relieved nor hot isostatically pressed [22].

There is another standard which specifically covers the measurement of elasticity moduli using uniaxial testing which is the ASTM-E111 [29], This test method, not used in the current work, consists of cycling the specimen within the elastic region for a minimum of three times before straining into the plastic range to get tensile yield and strength. This standard highlights the importance of factors which affect the use of uniaxial testing, including clamp effect and specimen alignment, but also requires larger minimum dimensions. Even taking these test procedures into account and trying to correct for them [30], it is clear that modulus measurement by uniaxial testing is not ideal for accurate measurement of Young's modulus [18].

There are other techniques for elasticity modulus measurement, which are non-destructive and can be used on the same MTS specimens which will could then also be used for tensile tests, efficiently contributing to a rapid testing program. These include ultrasound [22] and thermomechanical analysers [31]. The ultrasound technique is known to be sensitive to grain size and impurities but more problematical is that the sample needs to be relatively thick. The thermomechanical analyser route on the other hand, which consists of a 1 Hz cyclical three point bending test with a small 2N load, seems more robust and promising as a test for Young's modulus, and will be tested by the authors as part of future work.

3.4. *YS, UTS, e_u and e_f comparison*

The 0.2% offset strain method was used to calculate the yield strength. As discussed in the previous section (Sec.3.3), the measured Young's Modulus are not consistent for different specimen dimensions, so it is necessary to establish to study the influence of Young's Modulus variation on the 0.2% offset YS values. Figure 5 shows DP800 stress–strain curves (strain values to 2%) of A50 and Mini2 specimens.

In the figure, the target range of DP800 YS values are based on automated plant measured data on A80 samples from Tata Steel. The results shows that measured Young's Modulus of Mini2 is much smaller than that of A50 standard specimen. However, this difference has negligible effect on the 0.2% offset YS values for the current cases. The 64.9% variance of Young's Modulus values result in 5.5% variance of YS values. All the YS values locate in the target range, even for the smallest DP800 YS obtained from the smallest dimension Mini2. This indicates the discontinuity of Young's Modulus will not affect the YS values much across the range of the current selected bar dimension.

Figures 6–8 show the UTS, YS, e_U and e_f results ranges of DP800, DP600 and 316L for different tensile bar dimensions, respectively.

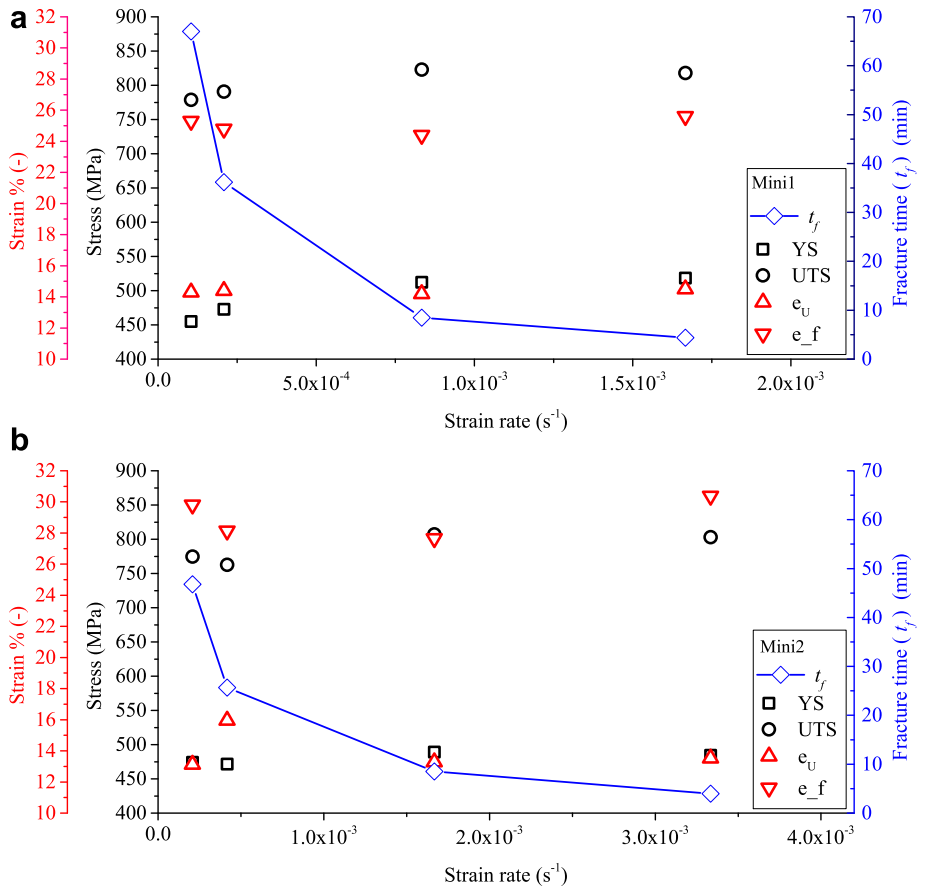

Fig. 3 – Influence of the strain rate on YS, UTS, uniform elongation (e_U), total elongation (e_f) and specimen fracture time (t_f) for DP800 Mini1 (*Top*) and Mini2 (*Bottom*) designs, respectively. The reported variables are not very sensitive to the strain rate variation in the range of 10^{-4} to 10^{-3} s^{-1}.

For DP800 and D600 (Fig.6 and Fig.7), the results show that result differences of the UTS, YS and e_U obtained from standard tensile specimens (A80, A50 and ASTM25) and the current designed non-standard dimension (Mini1 and Mini2) are small. However, some result differences were observed for 316L steel (Fig. 8). This is due to the tensile specimen manufacturing method. EDM method was used for DP800 and DP600 and AM method was adopted for 316L steel. Therefore, some defects, e.g. porosity, could influence the UTS, YS and e_U values. For all the cases, the total elongation increases as the specimen dimension is decreased. This is due to the differences of the aspect ratios for each design which will be discussed later. Table 4 shows The absolute value differences between averaged Mini2 and A80 test outputs of UTS, YS, e_U and e_f for DP800, DP600 and 316L steel, respectively.

These results further show the levels of the result variation between non-standard Mini2 and standard A80 dimensions.

Figure 9 shows result difference (*RD*) of UTS, YS, e_U and e_f in percentage between A50/ASTM25/Mini1/Mini2 and A80 for DP800 (*Top*: L-bar), DP600 (*Middle*: L-bar) and 316L (*Bottom*), respectively.

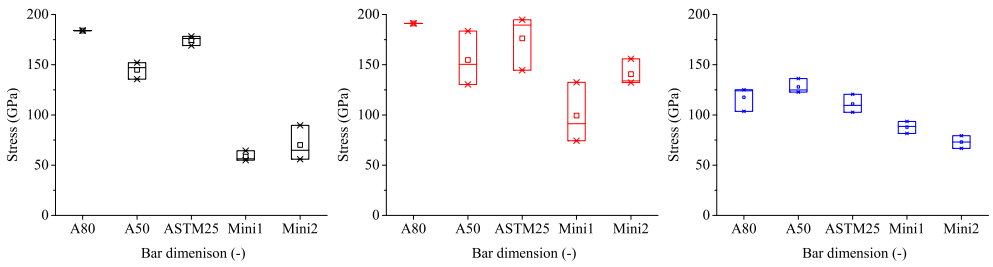

Fig. 4 – The measured Young Modulus *v.s.* specimen dimensions for DP800 (in black, *Left*), DP600 (in red, *Middle*) and 316L steel (in blue, *Right*), respectability. Young Modulus are hard to capture precisely, especially for the miniaturized specimens. In the box-plot figure, the ×, □ and – represent the data limit (both upper and lower), the mean and the median of the data, respectively.

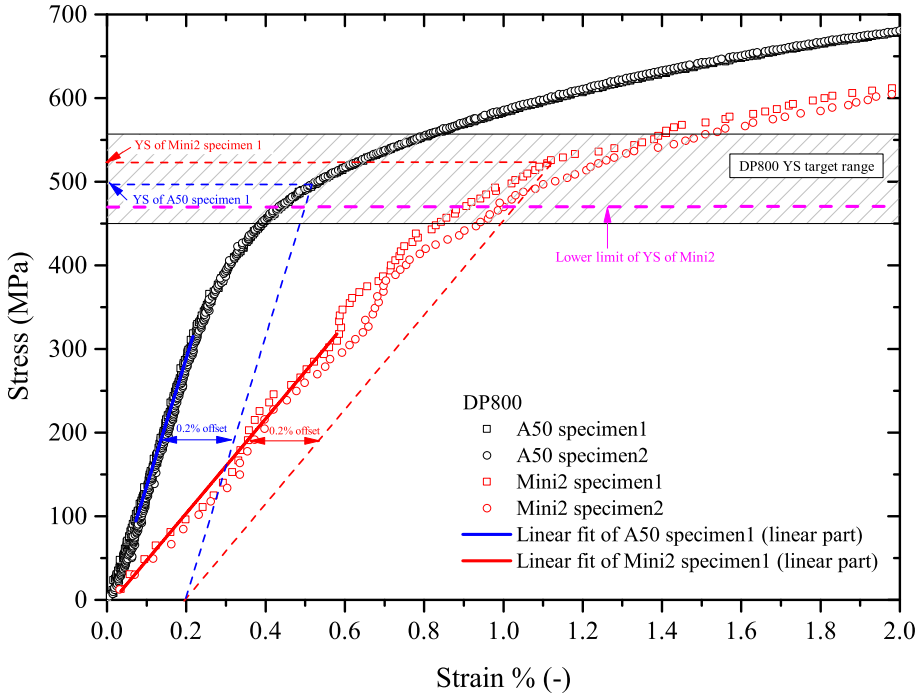

Fig. 5 – DP800 stress–strain curves of A50 (in black) and Mini2 (in red). Lower value of Young's Modulus is not necessarily results in lower value of YS.

The results indicate that even for the standard dimensions (A80, A50 and ASTM25), there are differences between the measured values. Notice that the difference between A80 and Mini2 is comparable to the difference between ASTM25 and the larger standard test pieces. For DP800, DP600 and 316L, the maximum *RD*% values, among UTS, YS and e_U, are in the ranges of −4.16%–13.9%, −7.71%–11.43% and −19.59%–14.03%, respectively.

In the work of Kashaev et al. [16], a similar (but not identical) tensile specimen dimension (named micro-tensile in

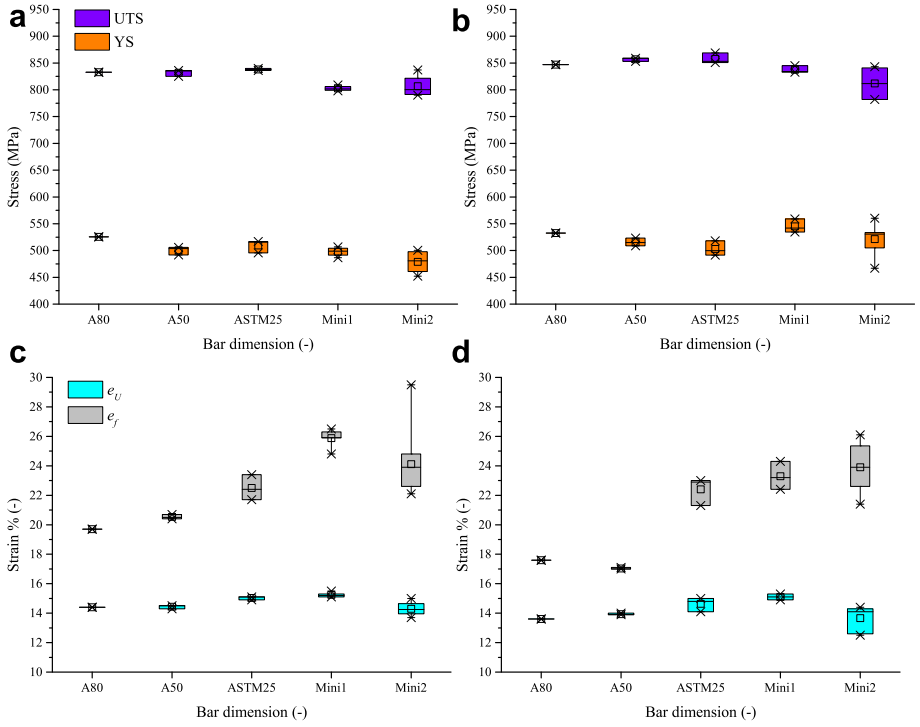

Fig. 6 – The UTS, YS, e_U and e_f result range of DP800 for different bar dimensions *Left*: L-bar and *Right*: T - bar. In the box-plot figure, the ×, □ and – represent the data limit (both upper and lower), the mean and the median of the data, respectively.

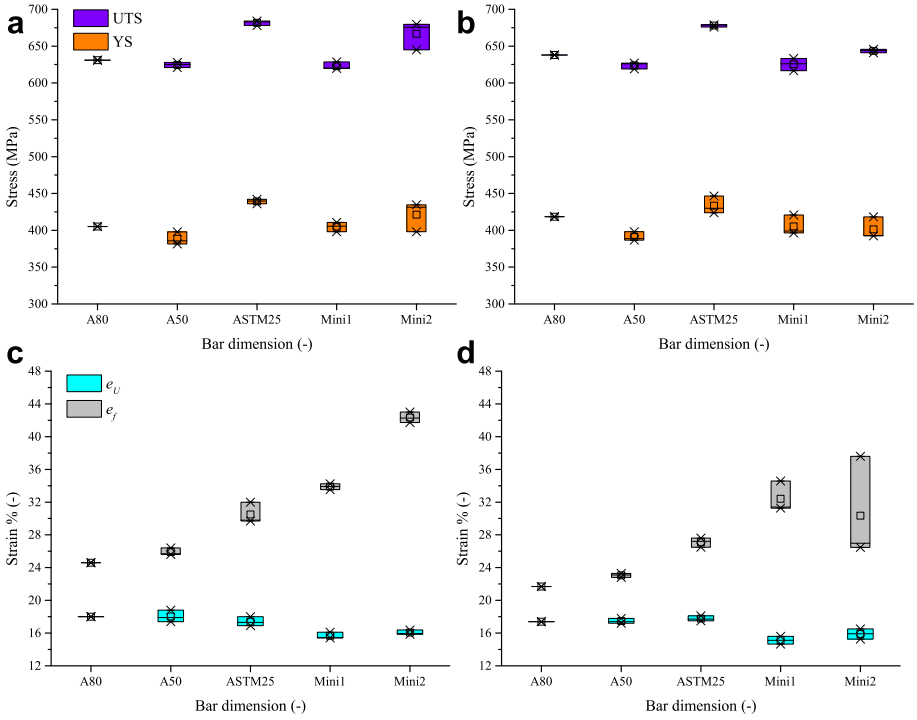

Fig. 7 – The UTS, YS, e_U and e_f result range of DP600 for different bar dimensions *Left*: L-bar and *Right*: T - bar. In the box-plot figure, the ×, □ and – represent the data limit (both upper and lower), the mean and the median of the data, respectively.

that work), compared to Mini2 in the current research, was adopted to study Inconel 625, 718 and Ti–6Al–4V alloys, respectively. The thickness of designed specimen is 0.5 mm. Also, another similar (also not identical) dimension (named miniature specimen in that work), compared to Mini2, was used to study the strength of CrMoV weldment by Yang et al. [18]. The thickness of was 1 mm in that work. Figure 10 shows the results difference percentages of the UTS and YS for different alloys in different research work.

The results difference percentages are calculated between the tensile results from the Mini2 (or similar) dimension tensile bar and from the standard tensile specimen (micro-tensile *v.s* ASTM E8 [16], Mini2 *v.s* ASTM25 and miniature specimen *v.s.* standard round bar [18], respectively). The results shows that compared to the work of Kashaev et al. and Yang et al., the results difference percentage of the current Mini2 design in the similar level of range, e.g. < 12%.

3.5. *Size effect on* e_f

The Bertella-Oliver formula [32] was used to convert the total elongations of different tensile specimen dimensions. The equations can be expressed as follows:

$$e = e_r \cdot \left(\frac{K_r}{K}\right)^n, \tag{1}$$

$$K_r = \frac{(L_0)_r}{\sqrt{(a_0)_r \cdot (b_0)_r}}, \tag{2}$$

and

$$K = \frac{L_0}{\sqrt{a_0 \cdot b_0}}. \tag{3}$$

In the equation, e and e_r are the total elongations of tensile specimens with slimness values K and K_r, respectively. The subscript r denotes the reference specimen dimension. L_0, a_0 and b_0 represent the gauge length, the thickness and the width of the parallel section of the tensile specimen, respectively. n is a constant depending on the material composition, for example, n values are 0.4 for carbon steel and 0.127 for austenitic stainless steels [26]. However, some limitations apply when using the those equations: the ratio of tensile bar width to thickness should smaller than 20 and the slimness ratio should be smaller than 25. By comparing these two limitation ratios to our extreme cases, we have 16.67 < 20 and 16.33 < 25. Therefore, the Bertella-Oliver formula is considered valid in the current work.

Figure 11 shows the total elongation variation with the tensile specimen slimness ratio K ($L_0/\sqrt{a_0 \cdot b_0}$) for DP800, DP600 and 316L, respectively.

The results indicate that the total elongation decreases as the slimness ratio values increase. The lines represent fits made using n values of 0.11 (in blue), 0.31 (in red) and 0.2 for 316L stainless steel, DP600 (L-Bar) and DP800 (L-Bar), respectively. The results show that a relatively good agreement was achieved by using these n values. This can help predict the total elongation with different specimen dimensions.

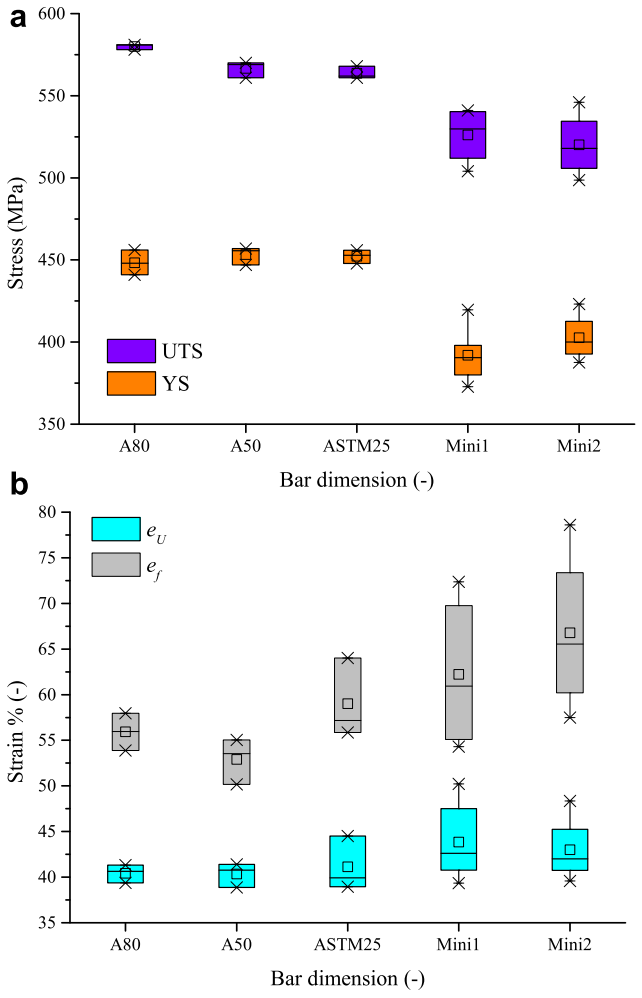

Fig. 8 – The UTS, YS, e_U and e_f result range of 316L steel for different bar dimensions. In the box-plot figure, the ×, □ and – represent the data limit (both upper and lower), the mean and the median of the data, respectively.

3.6. *Fractography analysis*

Fracture surfaces of ASTM25 specimen were investigated using scanning electron microscopy (SEM). Figure 12 shows the wide view and higher magnification images of fractured surfaces (parallel to the loading axis) and as-received materials' microstructures in the rolling direction (RD) cross-sectional view of commercial DP600 steel sheets.

Both materials have a uniform dispersion of a second phase martensite and a fraction of bainite (indicated by arrow in Fig. 12 (c)). Banding features are also visible in both materials, form along the rolling direction due to segregation of alloying additions in commercially manufactured steels.

Table 4 – The absolute value differences between averaged Mini2 and A80 test outputs of UTS, YS, e_U and e_f for DP800, DP600 and 316L steel, respectively.

		ΔUTS (MPa)	ΔYS (MPa)	Δe_U (–)	Δe_f (–)
DP800	L-bar	34.89	51.49	1.28	4.41
	T-bar	33.88	29.74	0.41	6.30
DP600	L-bar	36.77	16.19	1.94	17.74
	T-bar	5.62	17.17	1.50	9.65
316L	–	57.24	44.77	2.88	6.09

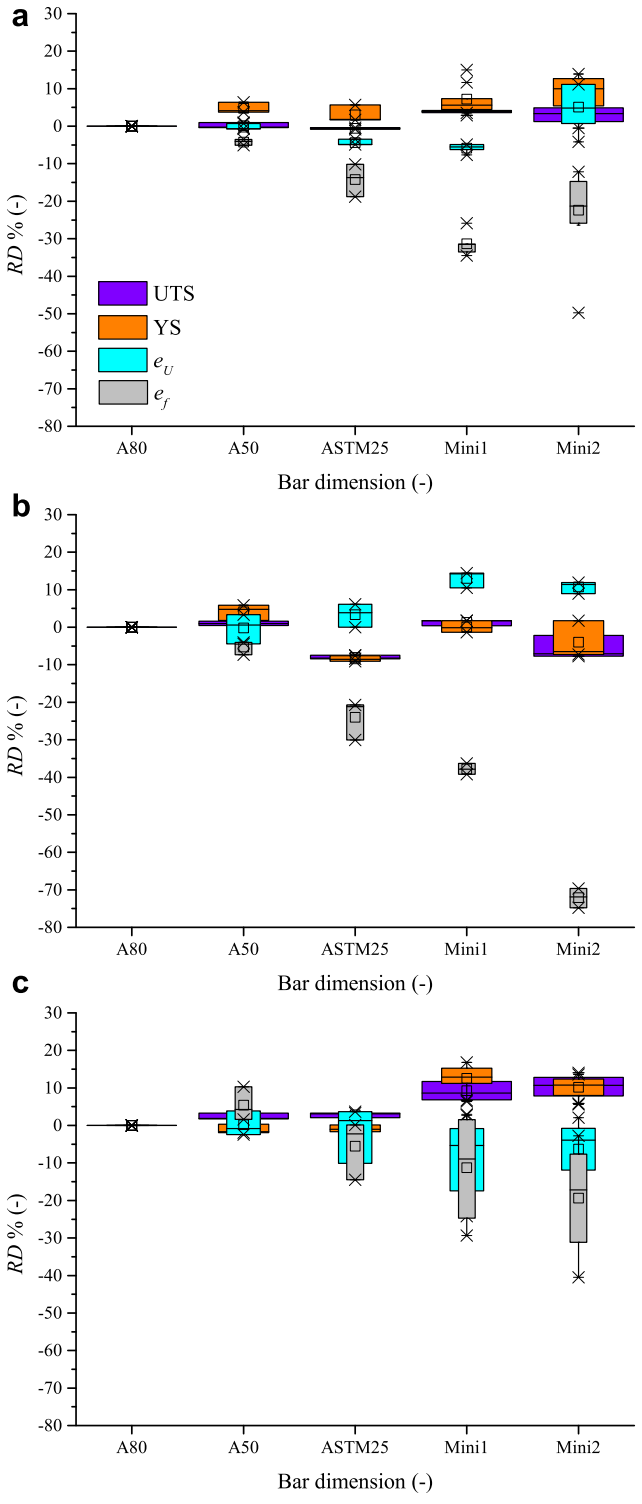

Fig. 9 – The result difference (*RD*) of UTS, YS, e_U and e_f in percentage between A50/ASTM25/Mini1/Mini2 and A80 for DP800 (*Top*: L-bar), DP600 (*Middle*: L-bar) and 316L (*Bottom*), respectively. In the box-plot figure, the ×, □ and – represent the data limit (both upper and lower), the mean and the median of the data, respectively.

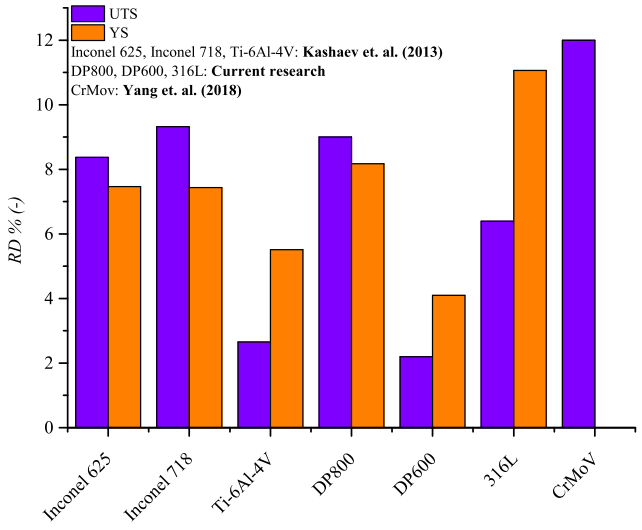

Fig. 10 – The results difference (*RD*) of the UTS and YS for different alloys.

DP800 shows significant banding as well as centreline segregations in the middle of sheet thickness (Fig. 12 (f)). The DP600 specimen (Fig. 12 (a)) has a smaller fracture surface area as compared to DP800 (Fig. 12 (d)), which indicates necking to a larger extent in DP600. This is in agreement with tensile test results where DP600 showed higher post-necking elongation until fracture. Both DP600 and DP800 steels show characteristic dimples (Fig. 12 (b), (e)), which imply a ductile fracture mode with localised deformation in the necking region. It also suggests microvoid formation and coalescence are the dominant fracture mechanisms, which is usual in tensile testing of those commercial dual phase steels [33,34]. Some deep and elliptical dimples are also seen which may be related to cracking of hard second phase (martensite) while the surrounding softer ferrite continues to deform until tensile fracture. A large cup-shape in the central region of a fracture surface and reduction in cross-section/thinning of specimen in necked regions (Fig. 12 (a) and (d)) may be caused by coalesce of voids in the central region.

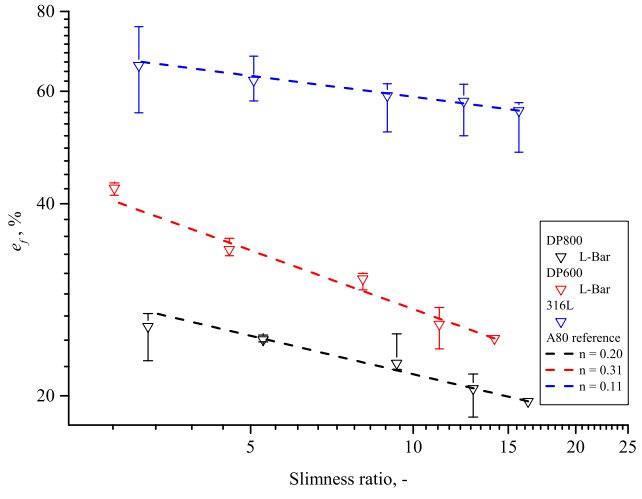

Fig. 11 – The total elongation *v.s.* tensile specimen slimness ratio ($L_0/\sqrt{a_0 \cdot b_0}$) for DP800, DP600 and 316L, respectively.

The fracture surface of small size 316L tensile specimen and the microstructure of as-built ALM material are presented in Fig. 13.

SEM analysis revealed large sized pores near the edges of the material (Fig. 13 (c)), as shown in a low magnification backscattered electron (BSE) image of a transverse cross-section prepared through the middle (gauge length region) of an as-built small size tensile bar. Figure 13 (d) reflects microstructure and melt pool tracks in the side-view plane, normal to the build direction. Fine sized gas bubbles in melt pools and shrinkage at grain boundaries were also observed in the areas away from the edges during SEM investigations, as shown in Fig. 13 (c) and (d) (indicated by arrows). ALM built 316L had the lowest tensile strength but much greater elongation compared to the DP steels and revealed many large and deep voids at the fracture surface (Fig. 13 (a), (b)). This may be attributed to the inherent porosity and shrinkage in the AM built material. Although, 316L shows the largest elongation from the stress–strain data this is not so apparent from fractography analysis. This discrepancy between apparent local brittle fracture behaviour and high global bulk ductility has been noticed before [23,24], and may be related to the laser spot size and high cooling rates affecting local microstructures and porosity during AM manufacture. 316L showed smaller necked cross sectional area and the largest total elongation.

For the three steels investigated, the additively manufactured 316L displayed the highest ductility with ε_f in excess of 50% for all tensile bar dimensions. This is due to the microstructure comprising of the inherently ductile face centred cubic (FCC) austenite phase. Both DP600 and DP800 contain both ferrite and martensite which have body centred cubic (BCC) and body centred tetragonal (BCT) structures respectively. These phases are both less ductile than austenite, resulting in lower ductilities observed for the dual phase steels.

4. Conclusions

In this research we proposed new designs of miniaturized tensile specimens (MTS) with smaller slimness ratios compared to the current standards for standard specimens. The effectiveness of the MTS was validated via experiments; covering three different alloys (DP800, DP600 and 316L stainless steel) and two manufacturing methods (Electrical Discharge Machining and Additive Manufacturing). The main conclusions can be summarized as follows:

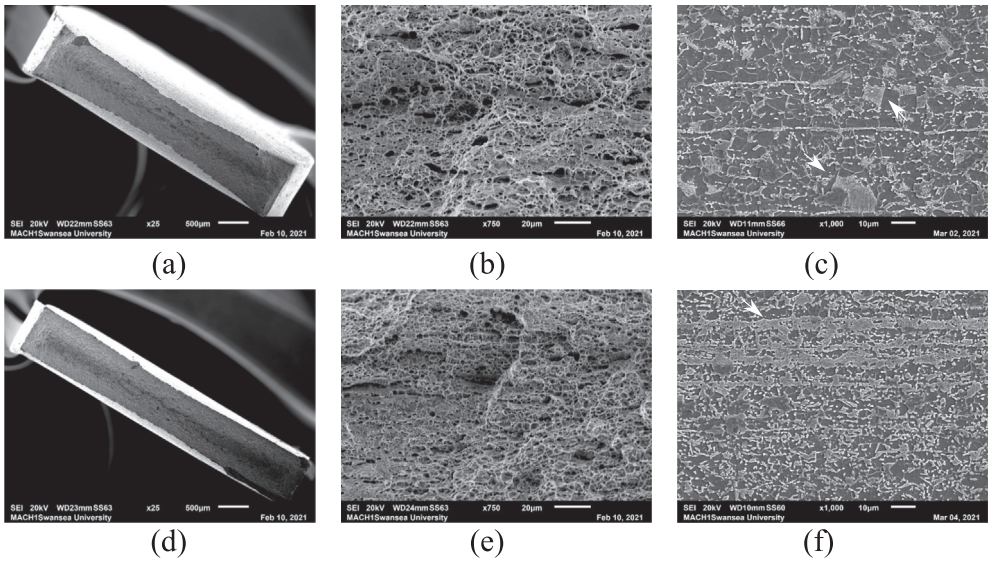

Fig. 12 – Overview (a, d) of fractured surfaces and magnified SEM (b, e) images of ASTM25 tensile specimens and as-received material microstructure in the rolling direction of DP600 (a–c) with arrows indicating bainite and DP800 (d–f), arrow indicating centreline segregations.

1. The current design of MTS, e.g. Mini2, can report consistent and repeatable tensile results for all the selected alloys for both manufacturing methods and in the case of DP steels rolling direction as well. This answered question 1 & 2 raised in Sec.1.
2. The tensile test results obtained from the current designed MTS with smaller slimness ratios can still represent bulk material properties. The maximum difference percentage ranges (between Mini2 and the baseline for the three different alloys) are −10.7%–5.5%, −11.3%–6.5% and

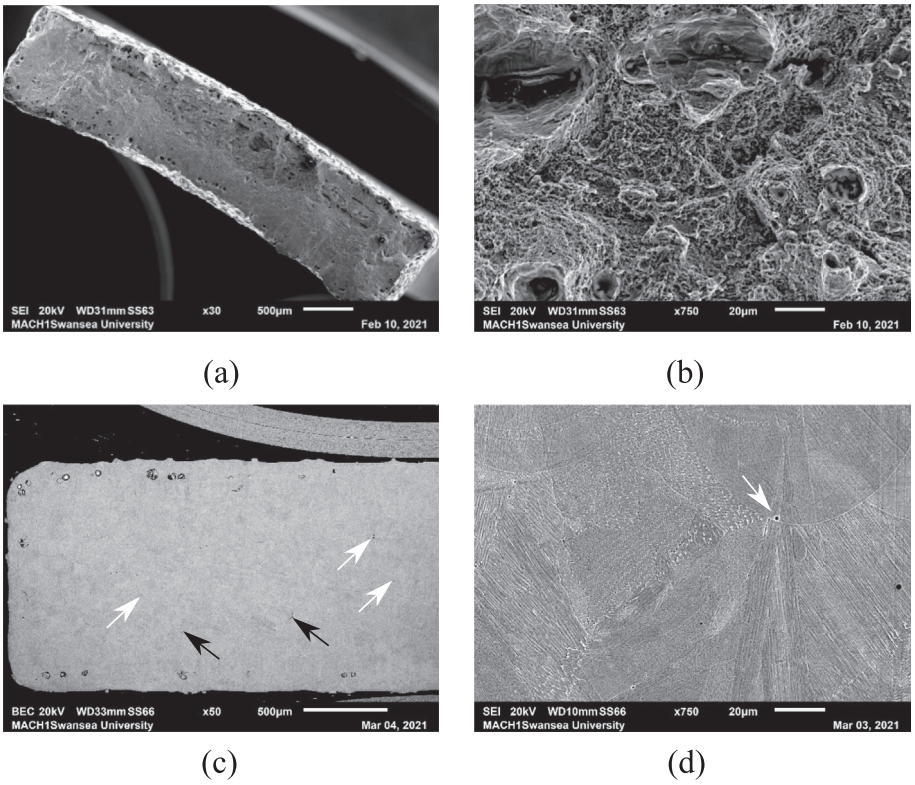

Fig. 13 – Fractured surface of tensile tested 316L ASTM25 specimen (a, b) and BSE image (c) from transverse cross-sectional view of as-built ALM 316L sample, while (d) microstructure in the side direction i.e. vertical to the build-direct (laser axis). White arrows indicate gas bubbles and black arrows for shrinkage at grain boundaries.

–11.1%–0.2% base on A80, A50 and ASTM25, respectively. This answered question 3 raised in Sec.1.
3. The designed MTS tensile test outputs are not so sensitive (less than 5%) to the strain rate in the current strain rate range. This answered question 4 raised in Sec.1.
4. The differences between miniature specimens and standard specimens are of the same order as the differences between the different standard specimens. This gives confidence in using these MTS geometries for characterising the mechanical properties of samples manufactured using a RAP process.
5. The Bertella-Oliver formula was used to convert the total elongations of different tensile specimen dimensions. The geometrically dependent constant (n) values are 0.2 and 0.31 for DP800 and DP600 alloys, respectively.

Further work will focus on the mechanical testing of the materials obtained through small scale Rapid Alloy Prototyping process by using Mini1/Mini2 design. A further study on the discontinuity of Young's Modulus and its technique improvement may also be interesting.

Declaration of Competing Interest

The authors declare that they have no known competing financial interests or personal relationships that could have appeared to influence the work reported in this paper.

Acknowledgements

The authors would like to thank EPSRC for funding the Rapid Alloy Prototyping Prosperity Partnership project (EP/S005218/1 - ACCELERATING ALLOY DEVELOPMENT THROUGH DELIVERING NOVEL PROTOTYPING SOLUTIONS) which made this work possible. The authors would also like to thank the Welsh Government, European Regional Development Fund (ERDF) and SMART Expertise Wales for funding Materials Advanced Characterisation Centre (MACH1) where the work was carried out.

REFERENCES

[1] Loveday MS, Gary T, Aegerter J. Tensile testing of metallic materials: a review. 2005.
[2] British Standards Institution. British Standard Method for a Tensile testing of metals (including aerospace materials). 1987, BS18.
[3] Lavery N, Mehraban S, Pleydell-Pearce C, Brown S, Jarvis D, Voice W, et al. Combinatorial development and high throughput materials characterisation of steels. Ironmak Steelmak 2015;42(10):727–33.
[4] Springer H, Raabe D. Rapid alloy prototyping: compositional and thermo-mechanical high throughput bulk combinatorial design of structural materials based on the example of 30Mn–1.2C–xAl triplex steels. Acta Mater 2012;60(12):4950–9.
[5] Farrugia D, Brown S, Lavery NP, Cameron P, Davis C. Rapid Alloy Prototyping for a range of strip related advanced steel grades. Proc Manuf 2020;50:784–90.
[6] Zheng P, Chen R, Liu H, Chen J, Zhang Z, Liu X, et al. On the standards and practices for miniaturized tensile test – a review. Fusion Eng Des 2020;161:112006.
[7] Jung P, Hishinuma A, Lucas GE, Ullmaier H. Recommendation of miniaturized techniques for mechanical testing of fusion materials in an intense neutron source. J Nucl Mater 1996;232:186–205.
[8] Zhu C, Xu J, Yu H, Shan D, Guo B. Size effect on the high strain rate micro/meso-tensile behaviors of pure titanium foil. J Mater Res Technol 2021;11:2146–59.
[9] Kohyama A, Hamada K, Matsui H. Specimen size effects on tensile properties of neutron-irradiated steels. J Nucl Mater 1991;179:417–20.
[10] Mikkelsen LP. Necking in rectangular tensile bars approximated by a 2-D gradient dependent plasticity model. Eur J Mech Solid 1999;18:805–18.
[11] Zhao Y, Guo Y, Wei Q, Dangelewicz A, Xu C, Zhu Y, et al. Influence of specimen dimensions on the tensile behaviour of ultrafine-grained Cu. Scripta Mater 2008;59:627–30.
[12] Kohno Y, Kohyama A, Hamilton ML, Hirose T, Katoh Y, Garner FA. Specimen size effects on the tensile properties of JPCA and JFMS. J Nucl Mater 2000;283–287:1014–7.
[13] Kula EB, Fahey NH. The effect of specimen geometry on determination of elongation in sheet tensile specimens. Technical report NO. Wal Tr; 1961. p. 111–26.
[14] ISO Standard 6892-1:2016. Metallic materials - tensile testing - Part 1: method of test at room temperature (BSI standard). 2016.
[15] ASTM E8/E8M-11. Standard test methods for tension testing of metallic materials. West Conshohocken, PA, USA: ASTM International; 2013.
[16] Kashaev N, Horstmann M, Ventzke V, Riekehr S, Huber N. Comparative study of mechanical properties using standard and micro-specimens of base materials Inconel 625, Inconel 718 and Ti-6Al-4V. J Mater Res Technol 2013;2(1):43–7.
[17] Dzugan J, Rund M, Prantl A, Konopik P. Mini-tensile specimen application for sheets characterization. IOP Conf Ser Mater Sci Eng 2017;179:012020.
[18] Yang B, Xuan FZ, Chen JK. Evaluation of the microstructure related strength of CrMoV weldment by using the in-situ tensile test of miniature specimen. Mater Sci Eng 2018;736:193–201.
[19] LaVan D, Sharpe W. Tensile testing of microsamples. Exp Mech 1999;39:210–6.
[20] Partheepan G, Sehgal D, Pandey R. An inverse finite element algorithm to identify constitutive properties using dumb-bell miniature specimen. Model Simulat Mater Sci Eng 2006;14:1433–45.
[21] Gussev MN, Busby JT, Field KG, Sokolov MA, Gray SE. Role of scale factor during tensile testing of small specimens. In: Sokolov M, Lucon E, editors. Small specimen test techniques: 6th volume. West Conshohocken, PA: ASTM International; 2015. p. 31–49.
[22] Santos RO, Silveira LB, Moreira LP, Cardoso MC, Silva FRF, Paula AS, et al. Damage identification parameters of dual-phase 600–800 steels based on experimental void analysis and finite element simulations. J Mater Res Technol 2019;8(1):644–59.
[23] Cherry JA, Davies HM, Mehmood S, Lavery NP, Brown SGR, Sienz J. Investigation into the effect of process parameters on microstructural and physical properties of 316L stainless steel parts by selective laser melting. Int J Adv Manuf Technol 2015;76:869–79.
[24] Lavery NP, Cherry JA, Mehmood S, Davies H, Girling B, Sacketta E, et al. Effects of hot isostatic pressing on the

elastic modulus and tensile properties of 316L parts made by powder bed laser fusion. Mater Sci Eng 2017;693:186–213.
[25] Aghadavoudi-Jolfaei M, Shen J, Smith A, Zhou L, Davis CL. Non-destructive measurement of microstructure and tensile strength in varying thickness commercial DP steel strip using an EM sensor. J Magn Magn Mater 2019;473:477–83.
[26] Davis JR. Tensile testing. ASM International Materials Park; 2004. OH 44073-0002.
[27] Cavusoglu O, Gural A, Gurun H. Influence of strain rate on tensile properties and fracture behaviour of DP600 and DP780 dual-phase steels. Ironmak Steelmak 2017;44(10):773–81.
[28] Lord JD, Rides M, Loveday MS. Modulus measurement methods, TENSTAND WP3 Report. National Physical Laboratory; Jan 2005.
[29] ASTM Standard E111-04, 2010. Standard test method for Young's modulus, tangent modulus and chord modulus. West Conshohocken, PA: ASTM International; 2010.
[30] Andras M. Effect of gripping system on the measured upper yield strength estimated by tensile tests. Measurement 2013;46(5):1663–70.
[31] National Institute of Standards and Technology National Construction Safety Team. Act report 1-3D. Natl Inst Stand Technol Natl Constr Sfty Tm Act Rpt 2005:1. 3D.
[32] Oliver DA. Proposed new criteria of ductility from a new law connecting the percentage elongation with size of test-piece. Proc Inst Mech Eng 1928;115(1):827–64.
[33] Kadkhodapour J, Butz A, Rad SZ. Mechanisms of void formation during tensile testing in a commercial, dual-phase steel. Acta Mater 2011;59:2575–88.
[34] Erdogan M. The effect of new ferrite content on the tensile fracture behaviour of dual phase steels. J Mater Sci 2002;37:3623–30.